Enhanced Oil Recovery as a second revenue stream in a gas storage facility; understanding and monitoring the Humbly Grove Field, Hampshire, UK

Arthur Satterley[1*], Potcharaporn Pongthunya[1], Jonny Imber[2], Ken McCaffrey[2], Jon Gluyas[2], Max Wilkinson[3], Andrew Sowter[4], Stefan Nielsen[2], Nicola de Paola[2], Richard Jones[3], Paul Jordan[5] and Arthur Moors[5] document the geological and flow modelling work conducted alongside safety monitoring – an essential part of gas storage operations.

Introduction

The Humbly Grove field is a unique example of an onshore UK field with two co-existing revenue streams. Its business model is based on oil production coupled with gas storage; relatively low-priced gas being stored in summer and produced at times of elevated demand and price in winter. After seasonal gas price variations were suppressed by imported LNG, Humbly Grove's oil production creates business resilience.

Gas is stored for customers by injecting it via the wells into the reservoir. The process continues until the storage facility is considered 'full'. When full, enhanced flow of oil into oil production wells is observed. This provides additional value that would not otherwise exist in a gas-only storage facility. As winter demand rises, or when gas is requested by customers, the process is reversed and gas is withdrawn from the reservoir. Traces of water, H_2S and other impurities picked up from the reservoir are removed to meet National Grid specifications and the gas is delivered to the network.

As with other gas storage facilities, Humbly Grove operates under strict national safety legislation. The licence to operate is dependent on a robust safety case. This was developed with an integrated approach to reservoir monitoring and modelling which combines a range of geoscience expertise to understand the behaviour and safe limits for gas storage.

History of the field

The Humbly Grove field (Figure 1) was discovered in 1980 by Carless Limited. Production began in 1984. Two oil-bearing reservoirs were discovered, both have gas caps; the shallower one in the Great Oolite Formation (late Bathonian) and a deeper reservoir in the Rhaetian Westbury Formation (late Triassic) which onlaps underlying hard, fractured Lower Carboniferous Limestone. Produced oil at surface had API gravity of 39° from the Great Oolite and 49° from the Rhaetian.

In 1999, Star Energy Limited acquired the field and commenced conversion to a gas storage facility. Between 1984 and 2005, with 20 wells, the field produced 5.9 MMbbl of oil and 8.7 Bcf of gas from the Great Oolite reservoir and 0.1 MMbbl of oil and 3.2 Bcf of gas from the Rhaetian reservoir. New surface facilities were installed, four gas storage wells were drilled into the gas cap of the Great Oolite and two into the gas cap of the Rhaetian reservoir.

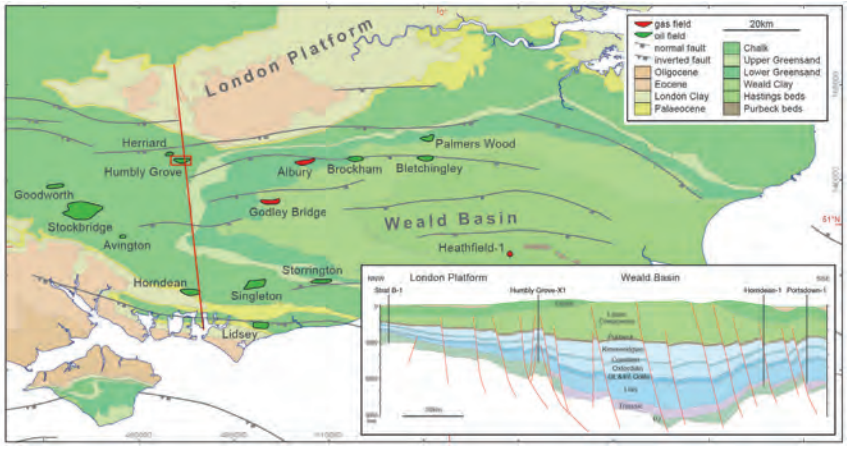

Figure 1 a) Humbly Grove location map (adapted from Sellwood et al. 1985, and Gluyas et al. 1985). The red line shows the location of the cross-section. The red rectangle is the outline of the Top Great Oolite depth map in Figure 3. The coordinate system is British National Grid; b) NNW-SSE cross-section showing the Humbly Grove structural high (from Gluyas et al., 2020).

[1] CGG, Reservoir Sciences | [2] Durham Energy Institute, Durham University | [3] Geospatial Research Ltd.
[4] TerraMotion Ltd. | [5] Humbly Grove Energy Ltd.
[*] Corresponding author, E-mail: arthur.satterley@cgg.com
DOI: 10.3997/1365-2397.fb2020069

The field operates within a defined operating range of gas volume and pressure. The gas inventory and field pressures are monitored to ensure the field remains well within defined operating limits.

The aim of this article is to document the geological and flow modelling work conducted alongside safety monitoring; an essential part of gas storage operations.

Geological model

The purpose of the geological model is to monitor reservoir pressure as part of site safety requirements and to provide a tool for operations monitoring and forecasting. It is also used for modelling future development options, including well abandonments, water disposal strategies, monitoring aquifer ingress and optimizing oil recovery. Seismic data are limited to 2D lines (Figure 2) and the resulting depth map (Figure 3) used with petrophysical data from logs and cores enables calculation of petroleum volumes in both reservoirs. The calculated volumes match the volumes estimated using material balance.

Original gas-oil and oil-water contacts are discernible using petrophysical interpretations. In addition, the field has a palaeo-oil-water contact identified from core data but without expression on wireline logs. Poroperm data were obtained every foot from 76 cores in 14 wells (Figure 4). The drop in permeability at 3393 feet tvdss is thought to be caused by an initial hydrocarbon charge filled to 3393 feet tvdss while diagenesis proceeded unhindered in the underlying aquifer. A second oil charge is inferred, although uplift associated with basin inversion (Butler and Pullan, 1990) could have caused gas exsolution from oil, gas cap growth and movement of the oil-water contact to 3595 feet tvdss, the initial field OWC in the Great Oolite reservoir.

Thus, the Great Oolite reservoir is vertically stratified. Above the palaeo-contact, porosity preservation is good and permeability high. Between 3393 feet tvdss and the initial oil-water contact at 3595 feet tvdss, reservoir properties are much poorer. Beneath the hydrocarbon zone, the aquifer is largely cemented and aquifer energy is low.

Progressive cementation in the aquifer was halted twice by hydrocarbon charge. Elsewhere in the Great Oolite of the Weald Basin, there is a similar relationship between reservoir properties and the timing of hydrocarbon charge (Trueman, 2003); the longer pore space remained filled with water, the worse the reservoir.

Original lithofacies within the Great Oolite are predominantly oolitic grainstones, frequently occurring as coarse-fine couplets. The top of the Great Oolite reservoir is cross-bedded and locally eroded. Sedimentary structures are typical of tidally influenced oolitic sand blankets (Ball, 1967). A marly, stylolitised, laterally continuous interval, the Hoddington Member, separates an upper from a lower reservoir zone. The diagenetic overprint is thought to be the main control on reservoir quality.

Well test permeability, production performance and slabbed core show evidence of a natural fracture network and larger-scale joint system in the Great Oolite. One image log was run in well HGA8Z. Natural, open fractures are common in the Great Oolite

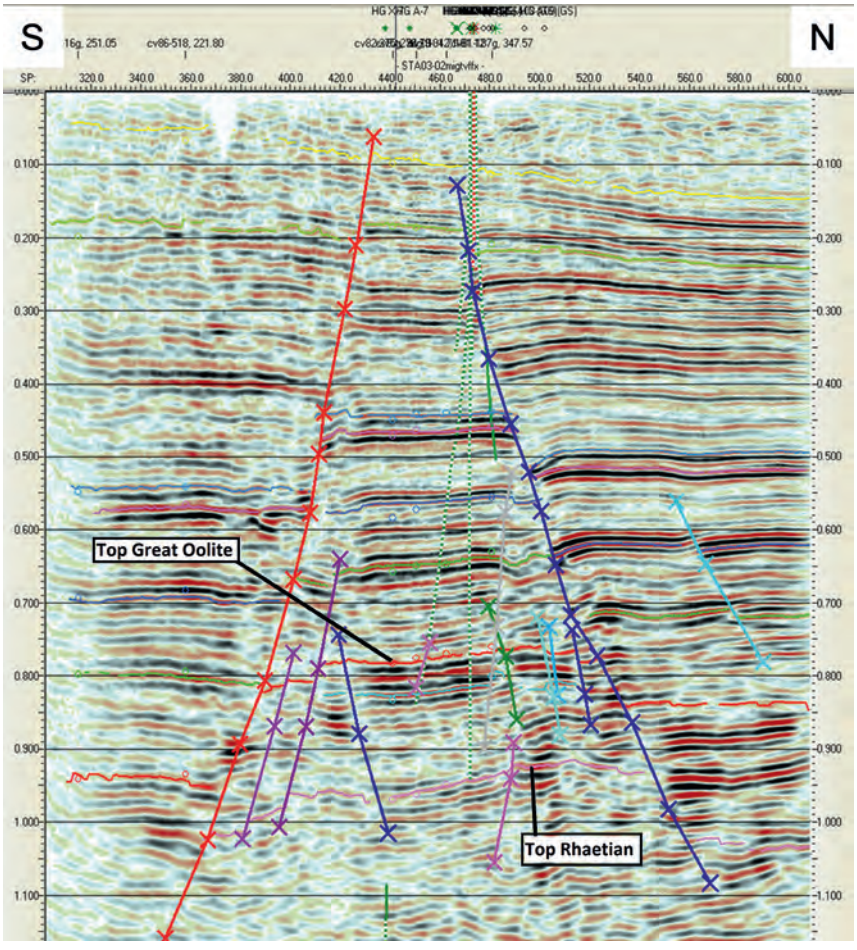

Figure 2 Seismic section through the Humbly Grove field, showing bounding faults and internal structures.

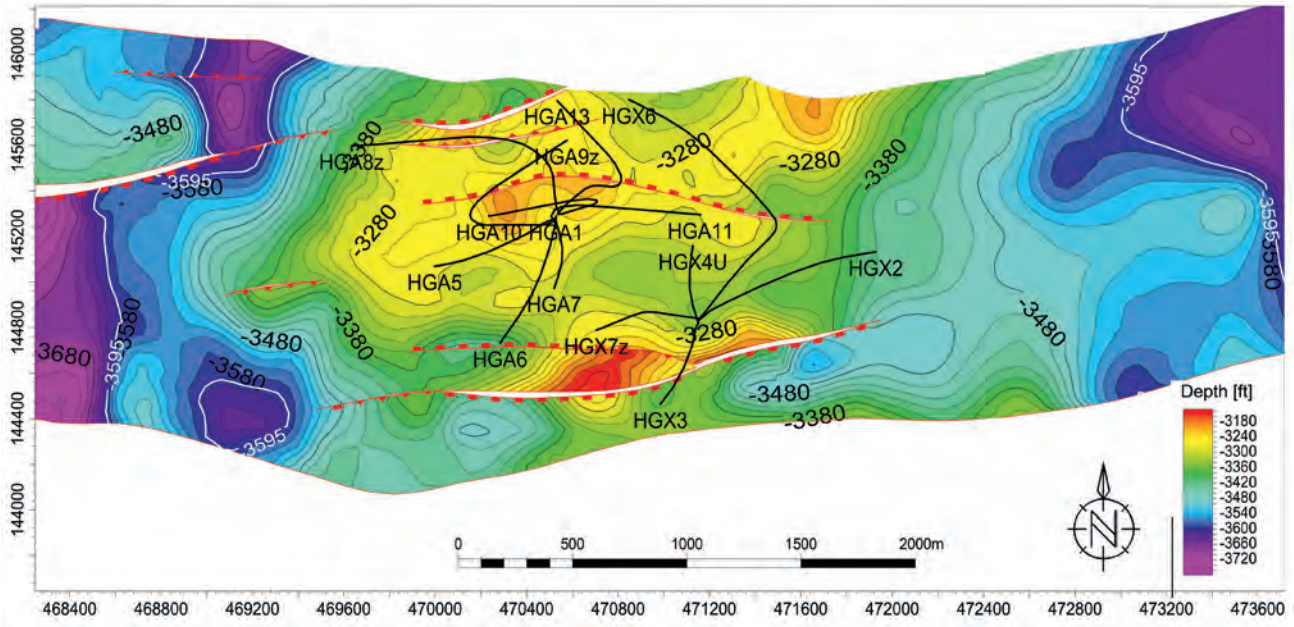

Figure 3 Depth structure map at the top of the Jurassic Great Oolite. (Map extends to the bounding faults only; oil-water contact at white contour). Coordinate system is British National Grid.

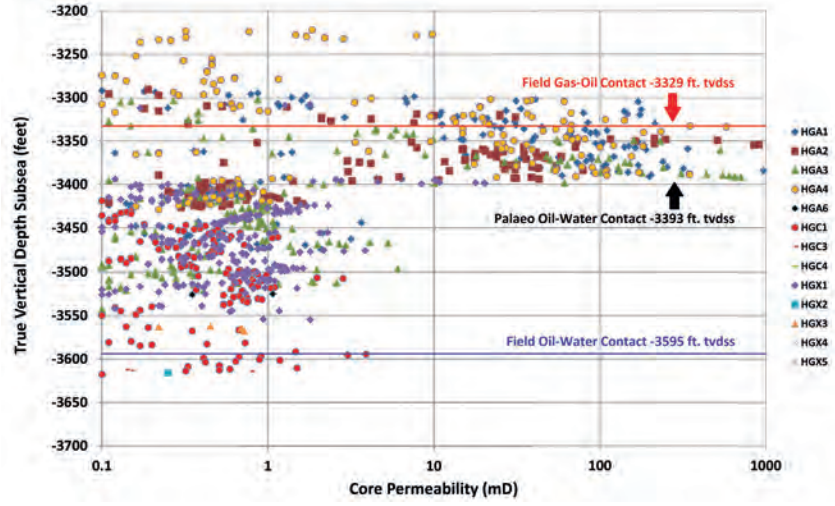

Figure 4 Palaeo-fluid contact, as seen in core plug permeability data plotted versus depth.

(Figure 5). Most are small with visible apertures between 0.1-0.5 mm. Lower-aperture fractures are hard to see in core and may be discernible using a microscope. These types of fractures may be responsible for higher than expected well test and production rates (given core plug permeability data).

Mud losses during drilling indicate scarce large and continuous fracture sets and are recorded largely between mapped faults, not at them. Early water breakthrough is not seen when wells cross faults.

Well test permeability in excess of core permeability is referred to as excess permeability and this information is used in the modelling work. Excess permeability values were mapped around the field, combined with mud loss event records and fracture intensity logs from core and the single image log. Resulting fracture intensity maps (by zone, Figure 6) form the basis of the fracture model. To these we apply estimated fracture permeabilities and then fracture porosity.

In the rock matrix, well test, production and core analysis data indicate considerable heterogeneity. A rock type model based on FZI methods was used to map reservoir quality in the field using core data (al-Ajmi and Holditch, 2000). Hydraulic Flow Units (HFU) were propagated from cored to uncored wells. The wide scatter of porosity – permeability plug data is resolved as tighter groupings that are mapped into the inter-well volume.

Matrix properties net-to-gross and porosity are mapped separately above and below the palaeo-oil-water contact. Permeability data are generated from porosity using Phi-K transforms for each HFU. Water saturation uses a saturation-height approach based on SCAL data and J-Functions, one function per HFU, including porosity and permeability terms.

Flow model and history match

An upscaled version of the fine geomodel was initialized in the simulator using measured oil and gas PVT, relative permeability curves for each HFU and for fractures (Figure 7). Initial reservoir pressure was 1495 psia; the field pressure history takes the form of occasional static bottom-hole pressure measurements. Pressure

responds much faster in the high-permeability zone above the palaeo-oil-water contact than in the low-permeability rock below. Initial model testing showed that a dual-porosity single-permeability set-up was the best initial description. A two-tank material balance model was used to condition the field performance as well as serving as a second field monitoring method alongside the flow simulation model.

Pressure was largely supported from 1984 to 2001 by gas re-injection. From January 2001, preparation for gas storage commenced as Star Energy began to blow down the gas caps causing major pressure depletion. Minimum field pressure was achieved in 2005 with the Great Oolite reservoir at c.600 psi compared with initial pressure of 1495 psi.

The history matching process started in June 1986, when the record of well daily rates began. History matching pressure variation and fluid rates in the production phase (1986-2005) at field and individual well level followed initialization. Comparing initial fluid distributions in the Great Oolite reservoir with those at the end of the production phase (1986 and 2005, Figure 7), the lack of aquifer movement is notable and the highly mobile gas

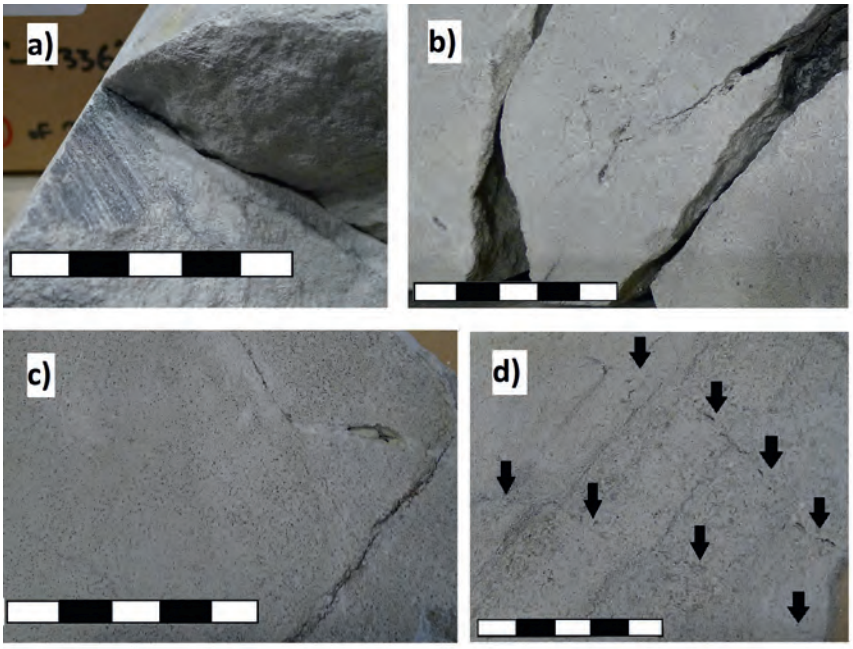

Figure 5 Fractures in Great Oolite core: a) Natural shear fracture exhibiting slickensides; b) open fractures in minor fault zone; c) sheared stylolite and open fracture; d) open hairline fractures. Scale bar: 5 cm.

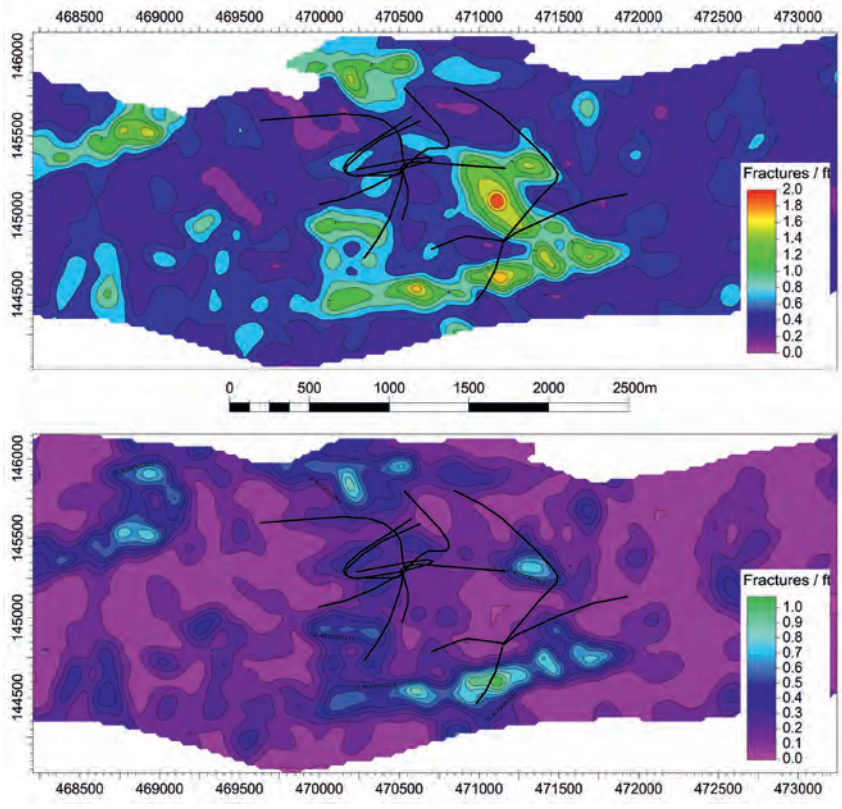

Figure 6 Fracture intensity maps for topmost Great Oolite zone (layered, more fractured) and Upper Great Oolite Reservoir Zone (massive bedding, less fractured). Coordinate system is British National Grid.

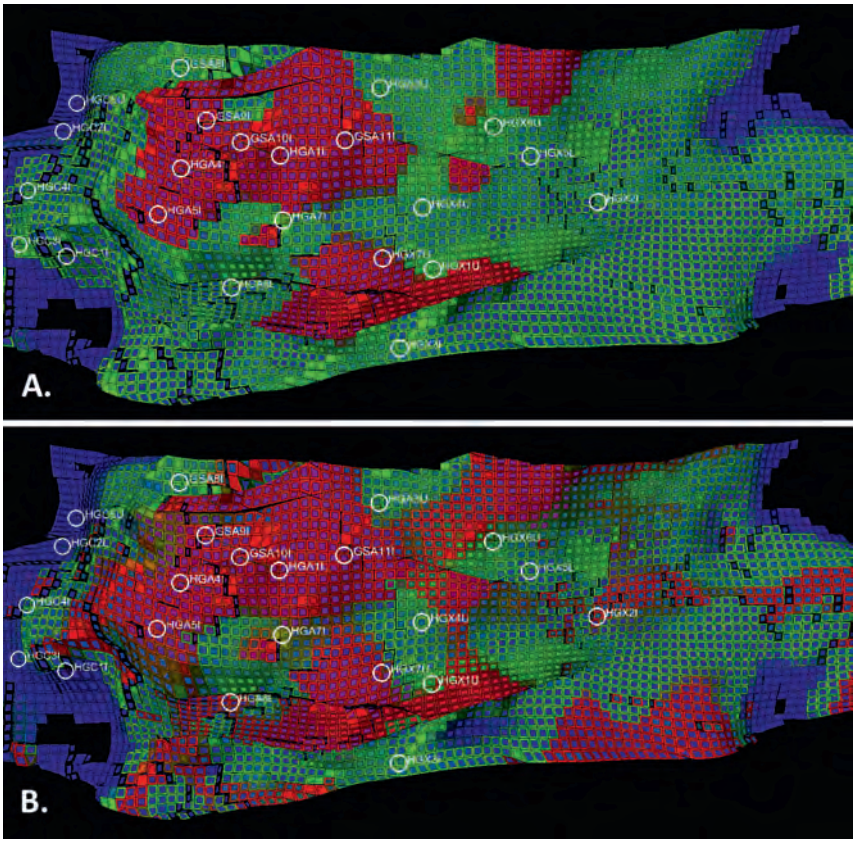

Figure 7 Great Oolite fluid saturation: a) Pre-production with 9 Bcf gas cap inventory; b) Immediately prior to commencement of gas storage, November 2005, when gas inventory was set at zero Bcf (gas red, oil green, water blue).

has migrated into pressure sinks caused by production from wells and produced gas reinjection.

History matching was achieved by adjusting fracture network permeability and fracture relative permeability end-points to control well rate, pressure and water breakthrough. Lateral connectivity of fracture sets to the aquifer is an unknown. Being the major permeability in the system, the fracture network properties around wells field-wide are the greatest dynamic uncertainty. Fine-tuning permeability in the low-permeability reservoir volume was necessary to achieve a good field pressure match.

Monitoring the main production and gas cap blowdown

Satellite-derived time series deformation (subsidence) plots for the Humbly Grove area between 1992 and 2009 were created. Data show the onset of a period of surface subsidence in the third quarter of 2001, apparently occurring after a time lag of circa six months from the onset of sustained pressure depletion by gas cap blowdown. Furthermore, time series deformation plots for specific sites in and around the facility exhibit different subsidence histories (Figure 8). Up to 10 cm of surface subsidence occurred along the southern margin of the Great Oolite reservoir and approximately 1.4 km east of the Hester's Copse well.

The clear temporal relationship between gas blowdown and surface subsidence suggests the following hypotheses: (1) an increase in vertical effective stress during blowdown led to compaction of the Great Oolite and Rhaetian reservoirs; and (2) subsidence was driven by reservoir compaction.

To test the hypothesis, a geomechanical model was constructed using data from unconfined uniaxial and confined triaxial rock tests, carried out on 12 samples of Great Oolite core, at the Rock Mechanics Laboratory, Durham University. Shale samples from the cap rock were too fragile to be cut, so model inputs for cap rocks use data available in the literature.

The data of fine-grained and coarse-grained oolites loaded to failure at Pc < 2900 psia can be fitted by a linear trend in accordance with the generic Mohr-Coulomb failure criterion. At confining pressure Pc > 2900 psia, the trend of the slope of the failure envelope gradually transitions into a ductile failure envelope with ductile failure occurring at constant shear stress. The value of peak stress under ductile deformation is difficult to evaluate within a few hundred psi but appears to be about 5220 psia for the coarse-grained, high-porosity samples and 4350 psia for the fine-grained, low-porosity samples.

An elastic dislocation model was then used (*Coulomb 3.3*; Toda et al., 2005, 2011; Lin and Stein, 2004) to test the second hypothesis by comparing the observed subsidence locations with predicted uplift/subsidence and Coulomb stress changes along the reservoir boundary faults (see King et al., 1994; Stein, 2003 for theoretical background).

A range of tested scenarios indicated that compaction amounting to ca. 0.5% vertical shortening in the Great Oolite reservoir or ca. 1.1% in the Rhaetian reservoir could generate the 10 cm of total subsidence observed in the time series deformation plots. It is inferred that compaction raised the Coulomb stress on a patch of the S-dipping boundary fault immediately below the Great Oolite reservoir. In turn, slip on this fault raised the Coulomb stress on a shallow patch of the N-dipping fault near Hester's Copse.

This hypothesis of fault reactivation during oil and gas production is consistent with evidence that faults in the vicinity

of Humbly Grove are critically stressed. Earthquake records and leak-off test data both support the notion that faults are critically stressed. No earthquakes were detected by the British Geological Survey during gas cap blowdown. Prior to production start-up, one natural earthquake occurred; a M_L = 3 earthquake on 19 July, 1982 with an epicentre 4 km to the southwest of Humbly Grove.

Leak-off test data indicate that the fracture gradient at Humbly Grove is within the range 2466 to 3046 psia km^{-1}. A leak-off test to failure from the Kimmeridge Clay in well HGB1 allows Mohr circles to be estimated for the likely range of stress states within the clay overburden. The Mohr circles plot close to, or intersect, the frictional sliding envelopes obtained from published data for clay-rich lithologies (Kholi and Zoback 2013; Bonnelye et al., 2016). Assuming these reactivation envelopes apply to Kimmeridge Clay, the *in situ* stress data support the hypothesis that optimally oriented faults were critically stressed when leak-off tests were performed.

From the above observations and interpretations, we infer that a small change in stress caused by reservoir compaction triggered slip along nearby, critically stressed, faults during gas cap blowdown from 2001 to 2005. The overburden at Humbly Grove contains the Oxford, Kimmeridge and Gault Clay formations. Deformation experiments on the Tournemire shale (Bonnelye et al., 2016) indicate that shale consistently exhibits brittle failure; stress drops and associated slips are slow and no acoustic emissions occur prior to failure (Bonnelye et al., 2017). Assuming that shales within the overburden at Humbly Grove are similar, we speculate that fault reactivation was accommodated by aseismic slip.

Gas storage and Enhanced Oil Recovery

Conversion to a gas store occurred in 2005. When moving from production to the storage phase of operations, relative permeability curves for the fracture network were modified so that the mobility of fluids in the fracture system reflected the different processes.

Material balance and static models indicate an original oil-in-place of approximately 38.8 MMbbl, of which 5.9 MMbbl was produced during the main production phase giving an oil recovery factor, with produced gas re-injection of 15.2% over 20 years.

During the gas storage phase, from 2005 to 2018, 0.87 MMbbl of oil was recovered, increasing the oil recovery factor to 17.5%. An oil enhancement programme was implemented in 2013. Enhanced surface facilities at the oil plant increased oil processing capacity. Oil production wells X4, X6 and X7 were re-tubed. The oil rate was increased from 200 BOPD to 700 BOPD.

The flow model is used to forecast remaining oil reserves with the support of well-by-well decline curve analysis which suggests that a further 0.81 MMbbl may be recovered (ultimate recovery 19.5%, 7.6 MMbbl).

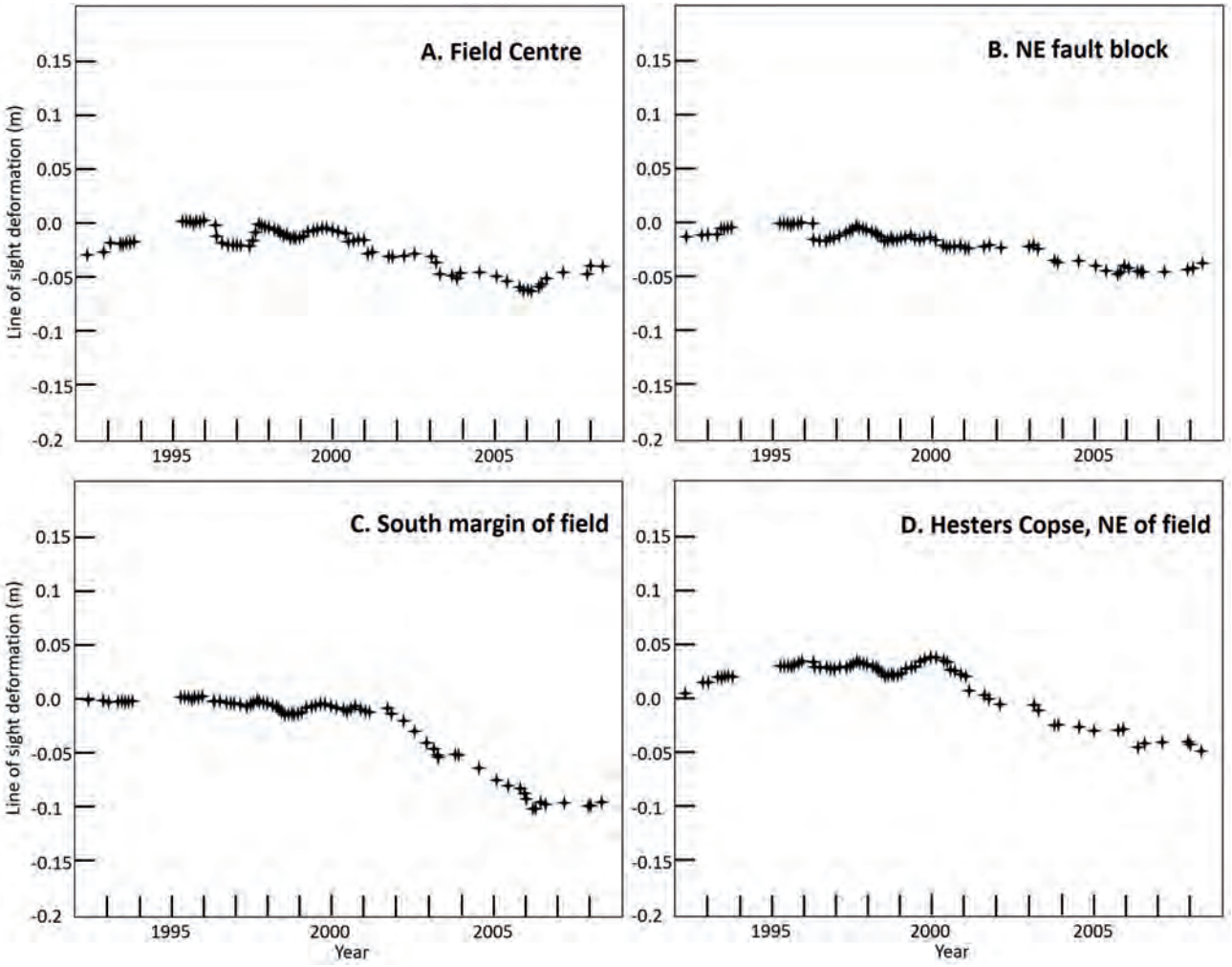

Figure 8 Satellite-derived time series deformation plots showing varied subsidence at specific locations over the period 1992-2009.

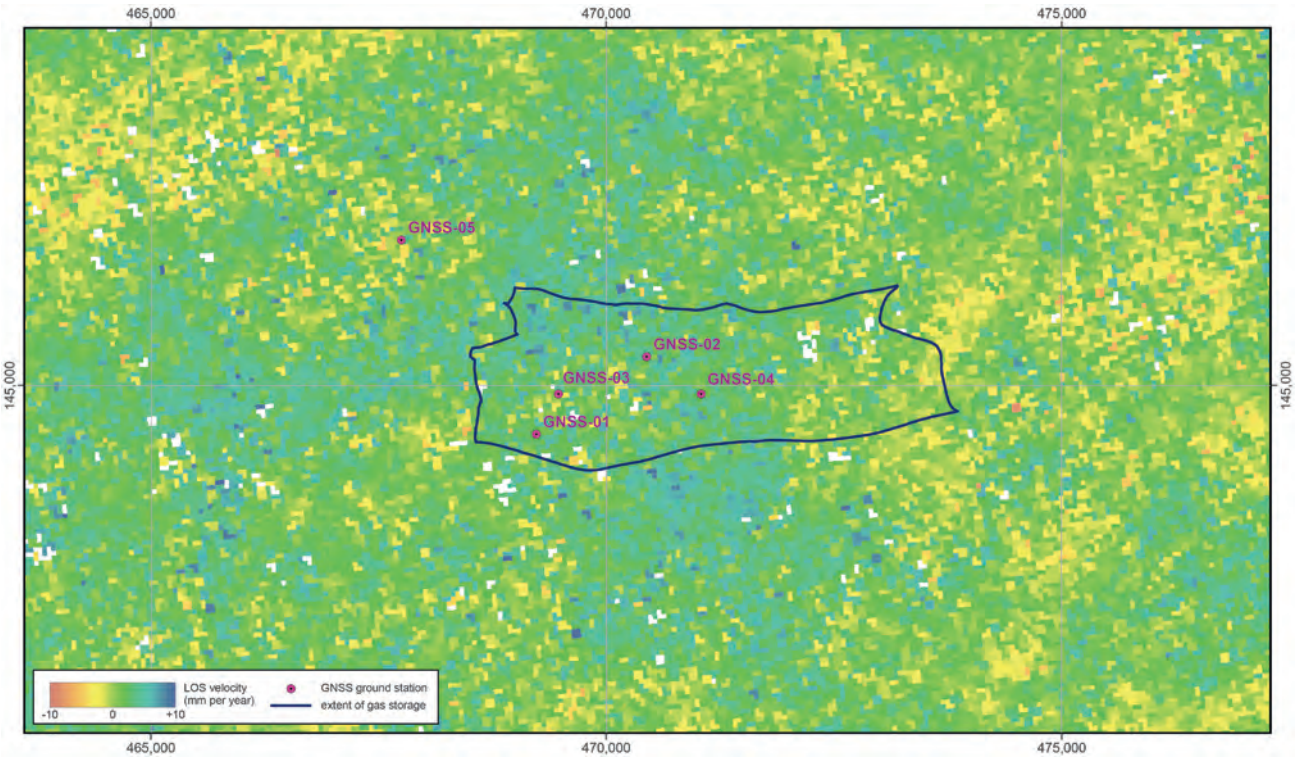

Figure 9 Average LOS velocity over Humbly Grove field between November 2014 and February 2017 measured using the ISBAS InSAR technique using Sentinel-1 satellite SAR data. (Coordinate system is British National Grid, grid spacing is 5 km).

Two oil production mechanisms are thought to be responsible for the enhanced oil recovery associated with gas storage operations. Rapid pressure depletion associated with winter gas withdrawal mobilizes some oil. High-rate gas injection forces gas into the high-permeability fractures from where it migrates into progressively lower-permeability rock at a distance from injector wells. Here, some gas dissolves in oil and this mobilized oil migrates into pressure sinks formed by operational oil-producing wells. Oil production is seasonal, typically reaching peak rate around full inventory and declining as the store is emptied. A key component of the EOR mechanism is miscible gas injection, whereby oil mobility increases as gas becomes dissolved into the oil at elevated pressures.

Simulation based forecasts offer optimized oil recovery options. Maximum oil recovery is achieved by means of a monthly pressurization and depletion cycle; however, this is incompatible with the current gas storage operation.

Aquifer influx and storage volume loss

During April to July 2016, the Rhaetian reservoir was left at low inventory for an abnormally long period and subsequent injection required the compressors to operate at maximum in order to inject 3 Bcf of gas. The flow simulator confirms strong aquifer influx as the likely cause and highlights the energy required at surface to counteract the aquifer once it has been allowed to advance.

Monitoring ground deformation during gas storage

Regular monitoring of the facility is required by the UK Oil and Gas Authority (OGA) and has entailed satellite- and ground-based monitoring, firstly by NPA (now CGG Satellite Mapping) and recently by Durham University Energy Institute. Several measurement techniques were deployed.

Firstly, satellite imaging has been a primary monitoring tool. Fifty-two descending synthetic aperture radar (SAR) images acquired between November 2014 and February 2017 were used to compute vertical surface deformation over time. An interferometric SAR (InSAR) analysis was performed using the intermittent small baseline subset (ISBAS) method (Sowter et al., 2013; Sowter et al., 2016) which is suitable for reservoir monitoring in vegetated terrain (Grebby et al., 2019).

The ISBAS InSAR analysis confirms that, on average, there was little to no significant motion over the site. Time series of motion for each of the 50 m pixels were calculated and these confirmed the result (Figure 9).

On the ground, terrestrial laser scanning (TLS) was deployed. This uses Lidar (Light Detection and Ranging) technology. The laser is fired in a sweep-mode to build a 3D image of an area. The hardware used has a range precision of 4-5 mm at 50-100 m. By conducting repeat surveys over time, 3D spatial changes to fixed objects can be detected (Wilkinson et al., 2010; 2012). TLS was carried out at five sites in March and then November 2016, i.e. covering final stages of winter gas production and the complete injection phase. Distances between fixed points on signs, buildings and electricity pylons were analysed for any displacements that might indicate ground movement.

Measured distance changes over c. 400 m length scales averaged 12 mm or less (near the detection limit of the hardware) compared with the initial survey. An absence of significant and systematic change suggests that ground movements are unlikely to have occurred between survey dates.

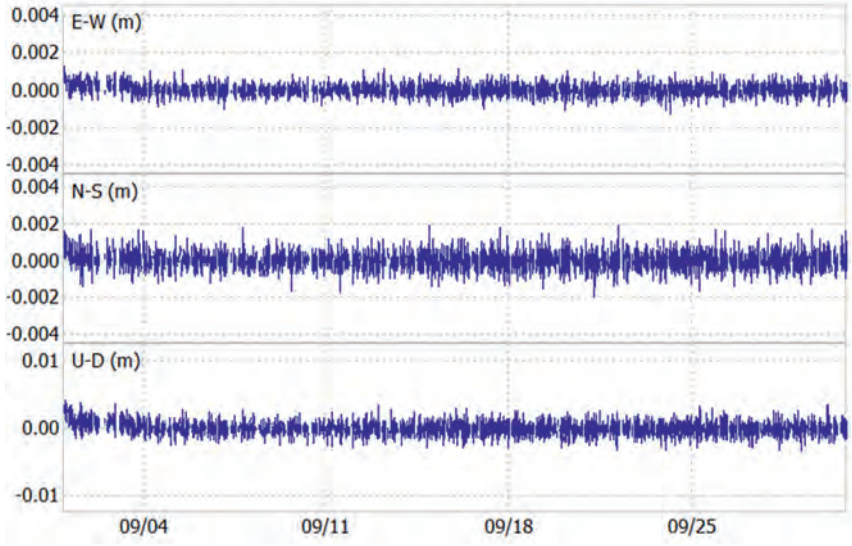

Figure 10 Example GNSS time series of position change of station GNSS-05 relative to station GNSS-01 for September 2016, presented in three components: east-west, north-south, up-down. The position data remains within the 2-3 centimetre precision of the method, is mostly flat-line and cannot be deemed significant.

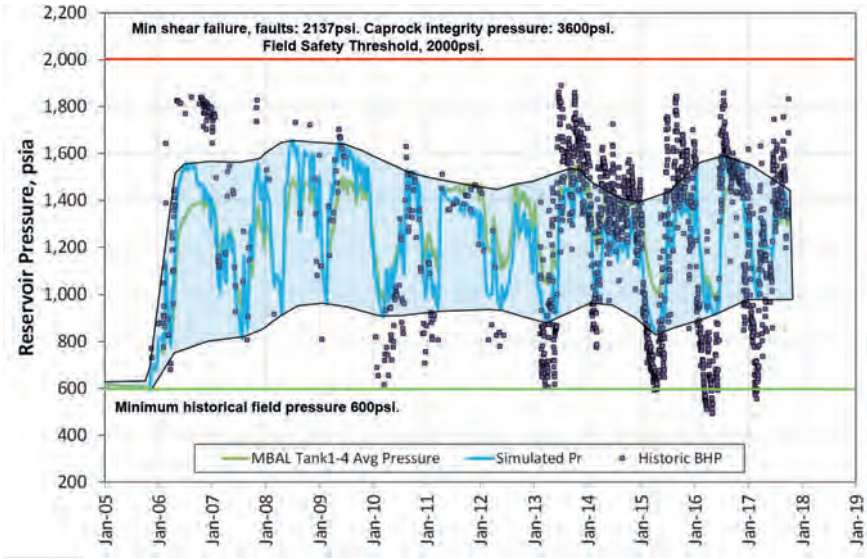

Figure 11 Gas store operating envelope, field average pressure (shaded) with bottom hole pressure data local to wells (points).

Global Navigation Satellite System (GNSS) stations were also installed at five well pad locations to continually monitor surface deformation at 15-second intervals from March 2016 to April 2017, spanning multiple injection and extraction cycles. A base station with fixed position allowed monitoring of surface deformation using relative positions of the remaining four stations.

Analysis of the time series revealed no movement between the five sites in excess of the 2-3 cm precision of the method (Figure 10). The lack of relative position change beyond measurement precision meant that we could not demonstrate deformation of the well pads relative to each other during the survey period.

Results of the current GNSS and InSAR studies indicate that there has been no detectable ground movement during gas storage. Considering the limits of resolution of the different monitoring methods, vertical ground motion (if any) during gas storage cycles is likely to be < 1 cm.

Returning to geomechanical modelling, the same elastic dislocation models described previously were used to place limits on the magnitude of reservoir compaction (or inflation) that occurs during gas storage, assuming that the overburden responds in an elastic manner. Predicted subsidence for a uniform vertical compaction of 0.012 m in the Great Oolite reservoir and 0.01 m in the Rhaetian reservoir generates a maximum surface subsidence of approximately 0.8 cm. This result suggests that any compaction (or inflation) of the reservoirs during gas storage amounts to < 0.04%, creating strain well below the expected elastic limit of the Great Oolite samples tested in the rock mechanics study. It is only during the substantial pressure depletion associated with gas cap blowdown in 2001-2005 that strains exceeded the limits on bounding faults.

Subsurface monitoring

Production, injection and pressure are monitored using the material balance model and flow simulator. Safe operating limits have been defined by geomechanical studies, and the field is operated well within these bounds. The Humbly Grove facility automatically cuts injection once 1682 psia wellhead pressure is reached, which corresponds to a maximum 1900 psia bottomhole pressure. Field average pressure is kept some 400-500 psia below the minimum shear failure pressure at faults. The flow simulation model monitors pressures in all forecasting work, thus ensuring continuing safety (Figure 11).

Consideration of faults in the subsurface indicates that they act as seals to the hydrocarbon accumulation and pass through thick overlying shale formations that isolate shallow, water-bearing, rocks from the gas store. Within the reservoir section, abundant small fractures allow compaction and stress release to occur within the confines of the reservoir without projecting strain associated with gas storage operations directly to bounding faults.

Conclusions

The Humbly Grove field in Hampshire, England represents an early example of the circular economy, in which equipment is repurposed and reused rather than scrapped. It has a greater degree of business resilience due to the combined revenues from oil production and gas storage which can serve as a model for the wider industry.

The two storage reservoirs are suited to gas storage as fracturing provides permeability, thus gaining good rate performance. In the Great Oolite reservoir, repressuring and gas miscibility mobilizes oil in an EOR process while aquifer ingress is weak. In the Rhaetian reservoir, fracturing and a strong aquifer require careful inventory monitoring particularly at low inventory to prevent pore volume loss when standing 'empty'.

In order to maintain the integrity of the storage site, comprehensive surface elevation monitoring has been undertaken and coupled with geomechanical and flow simulation modelling of the storage reservoirs. A wide range of geoscience expertise has been brought together to gain a good understanding of the reservoir behaviour and to help define safe operating protocols for the field alongside subsurface pressure and inventory monitoring.

Acknowledgements

The authors would like to thank Humbly Grove Energy Ltd. for its kind permission to show this work. They also thank their respective employers for permission to publish this article and to Richard Jones for his work in preparing figures.

References

Al-Ajmi, F.A. and Holditch, S. [2000]. Permeability Estimation Using Hydraulic Flow Units in a Central Arabia Reservoir. *SPE Annual Technical Conference and Exhibition*, SPE63254.

Ball, MM. [1967]. Carbonate sand bodies of Florida and the Bahamas. *Journal of Sedimentary Petrology*, **37**, 556-591.

Bonnelye, A., Schubnel, A., David, C., Henry, P., Guglielmi, Y., Gout, C., Fauchille, A.-L. and Dick, P. [2016]. Elastic wave velocity evolution of shales deformed under uppermost crustal conditions. *Journal of Geophysical Research: Solid Earth*, **122**, 130-141, doi:10.1002/2016JB013540.

Bonnelye, A., Schubnel, A., David, C., Henry, P., Guglielmi, Y., Gout, C., Fauchille, A.-L. and Dick, P. [2017]. Strength anisotropy of shales deformed under uppermost crustal conditions. *Journal of Geophysical Research: Solid Earth*, **122**, 110-129, doi: 10.1002/2016JB013040.

Butler, M. and Pullan, C.P. [1990]. Tertiary structures and hydrocarbon entrapment in the Weald Basin of southern England. In: Hardman, R.F.P. and Brooks, J. (eds]. Tectonic Events Responsible for Britain's Oil and Gas Reservoirs. *Geol. Soc. Lond. Special Publication*, **55**, 371-391.

Gluyas, J.G., De-Paola, N., Imber, J., Jezierski, T.M., Jones, R.R., Jordan, P., McCaffrey, K., Nielsen, S., Pongthunya, Y., Satterley, A., Sowter, A., Wilkinson, M. and Moors, A. [2020]. The Humbly Grove, Herriard and Hester's Copse Field, UK Land, In: Gluyas, J.G. and Goffey, G. (eds) UK Oil and Gas Fields, *Geological Society Memoir 52* (*in press*).

Grebby, S., Orynbassarova, E., Sowter, A., Gee, D. and Athab, A. (2019]. Delineating ground deformation over the Tengiz oil field, Kazakhstan, using the Intermittent SBAS (ISBAS) DInSAR algorithm. *International Journal of Applied Earth Observation and Geoinformation*, ***81***, 37-46. Doi:10.1016/j.jag.2019.05.001.

King, G.C.P., Stein, R.S. and Lin, J. [1994]. Static stress changes and the triggering of earthquakes. *Bulletin of the Seismological Society of America*, **84**, 935-953.

Kohli, A.H. and Zoback, M.D. [2013]. Frictional properties of shale reservoir rocks. *Journal of Geophysical Research: Solid Earth*, **118**, 1-17, doi:10.1002/jgrb.50346.

Lin, J. and Stein, R.S. [2004]. Stress triggering in thrust and subduction earthquakes, and stress interaction between the southern San Andreas and nearby thrust and strike-slip faults. *Journal of Geophysical Research*. **109**, B02303, doi: 10.1029/2003JB002607.

Sellwood, B.W., Scott, J.D., Mikkelson, P.W., Akroyd, P. [1985]. Stratigraphy and sedimentology of the Great Oolite Group in the Humbly Grove Oilfield, Hampshire. *Marine and Petroleum Geology*, **2**, 44–55.

Sowter, A., Bateson, L., Strange, P., Ambrose, K. and Syafiudin, M.F. [2013]. DInSAR estimation of land motion using intermittent coherence with application to the South Derbyshire and Leicestershire coalfields. *Remote Sensing Letters*, **4** (10), 979-987. Doi:10.1080/2150704X.2013.823673.

Sowter, A., Amat, M.B.C., Cigna, F., Marsh, S., Athab, A. and Alshammari, L. [2016]. Mexico City land subsidence in 2014–2015 with Sentinel-1 IW TOPS: Results using the Intermittent SBAS (ISBAS) technique. *International Journal of Applied Earth Observation and Geoinformation*, **52**, 230-242. Doi:10.1016/j.jag.2016.06.015.

Stein, R.S. [2003]. Earthquake conversations. *Scientific American*, **288**, 72-79.

Toda, S., Stein, R.S., Richards-Dinger, K. and Bozkurt, S. [2005]. Forecasting the evolution of seismicity in southern California – animations build on earthquake stress transfer. *Journal of Geophysical Research*, **110**, B05S16, doi:10.1029/2004JB003415.

Toda, S., Stein, R.S., Sevilgen, V. and Lin, J. [2011]. Coulomb 3.3 Graphic-rich deformation and stress-change software for earthquake, tectonic, and volcano research and teaching – user guide, US. *Geological Survey Open-File Report 2011-1060*, 63, http://pubs.usgs.gov/of/2011/1060/.

Trueman, S. [2003]. The Humbly Grove, Herriard, Storrington, Singleton, Stockbridge, Goodworth, Horndean, Palmers Wood, Bletchingley and Albury Fields, Hampshire, Surrey and Sussex, UK Onshore. In: Gluyas, J.G. and Hichens, H.M. (eds), United Kingdom Oil and Gas Fields, *Commemorative Millennium Volume*. Geological Society, London, Memoir, **20**, 929–941.

Wilkinson, M., McCaffrey, K.J.W., Roberts, G.P., Cowie, P.A., Phillips, R.J., Michetti, A., Vittori, E., Guerrieri, L., Blumetti, A.M., Bubeck, A., Yates, A. and Sileo, G. [2010]. Partitioned postseismic deformation associated with the 2009 Mw 6.3 L'Aquila earthquake surface rupture measured using a terrestrial laser scanner. *Geophysical Research Letters*, **37**, L10309.

Wilkinson, M.W., McCaffrey, K.J.W. , Roberts, G.P. Cowie, P.A. Phillips, R.J., Degasperi, M. Vittori, E. and Michetti, A.M. [2012]. Distribution and Magnitude of Post-seismic Deformation of the 2009 L'Aquila 1 Earthquake (M6.3) Surface Rupture Measured Using Repeat Terrestrial Laser Scanning. *Geophysical Journal International*, **189** (2), 911-922.